Instability of non-Newtonian jets with a surface tension gradient

2009 J. Phys. A: Math. Theor. 42 065501

(http://iopscience.iop.org/1751-8121/42/6/065501)

IOP PUBLISHING JOURNAL OF PHYSICS A: MATHEMATICAL AND THEORETICAL

J. Phys. A: Math. Theor. **42** (2009) 065501 (14pp) doi:10.1088/1751-8113/42/6/065501

Instability of non-Newtonian jets with a surface tension gradient

Zhanjun Gao

Kodak Research Laboratories, Eastman Kodak Company, Rochester, NY 14650-2121, USA

Received 12 September 2008, in final form 7 November 2008
Published 14 January 2009
Online at stacks.iop.org/JPhysA/42/065501

Abstract

In this paper we investigate the mechanisms of temporal instability of non-Newtonian liquid jets, more specifically viscoelastic liquid jets, with a surface tension gradient. The dispersion relation between the growth rate and the wave number for a viscoelastic liquid jet is derived. The effects of various parameters on the instability behavior are studied. A number of quantitative conclusions and sensitivities on the instability behavior of viscoelastic jets are investigated. The present work can provide a good foundation for further investigations of the instability and breakup of viscoelastic liquid jets in the situation where the surface tension gradient exists. The applications of such a phenomenon include a microfluidic inkjet printheads with thousands of nozzles that are thermally modulated near the nozzle orifice to produce steady steams of picoliter-sized droplets at kilo-Hertz frequency rates.

PACS number: 47.20.−k

(Some figures in this article are in colour only in the electronic version)

1. Introduction

Modern developments in the design and utilization of microfluidic devices for fluid transport have found many applications such as drug design and diagnostic devices in biomedicine and microdrop generators for image printing. Therefore, it is of interest and importance to understand the mechanisms of instability and breakup of liquid jets, as the efficiency and quality of production is strongly dependent on these mechanisms. The capillary instability of liquid jets has been the subject of numerous studies since the19th century. Rayleigh considered the breakup of an inviscid cylindrical jet into drops [1, 2]. He used a reference system wherein the cylinder of liquid was initially at rest and the perturbation applied was spatially periodic. Under appropriate circumstances, surface tension forces broke the liquid into equally spaced drops. Rayleigh then applied the conclusions to a moving jet of liquid emanating from a nozzle. In his work on drop formation Rayleigh linearized his equations by assuming the variation of the jet radius to be very small compared to the radius itself. This assumption

becomes invalid, of course, as drop separation occurs. Nonetheless, Rayleigh's work has given much insight into the phenomenon of liquid jet breakup. A one-dimensional model of drop separation has been used for the purpose of better understanding the jet breakup process [3]. In this model, the variables depend on the axial coordinate of the jet and on time. In using such a model, one assumes that the wavelength of perturbations on the stream is large compared to the radius (see, for example, [4]). Lee [3] considered the resulting nonlinear equations, avoiding the low amplitude assumption made by Rayleigh. Using numerical methods his results show the formation of satellite droplets as well as the main drops.

Notable examples of jet breakup include the jet experiments of Rutland and Jameson [5] as well as those of Goedde and Yuen [6] for water jets and of Kowalewski [7] for jets of high-viscosity fluids. A momentous paper by Peregrine *et al* [8] not only helped to crystallize some of the theoretical ideas, but also contained the first high-resolution pictures of water falling from a faucet.

Nonlinear studies have been carried out by Yuen [9] and later by Chaudhary and Redekopp [10]. A review of the subject can be found in Bogy [11], while recent simulations using boundary integral techniques are described in Mansour and Lundgren [12]. Viscosity-dominated flows form a separate but parallel field. Tomotika [13] considered the linear stability of a stationary cylindrical thread of viscous fluid surrounded by a second viscous fluid with surface tension acting at the interface. Qualitatively, the stability results are similar to inviscid studies with a maximally growing wave of the order of the unperturbed thread radius. A more complete theory, including the effects of nonuniform jet velocities can be found in Chandrasekhar [14], where it is shown that capillary instability provides linearly growing waves that scale the jet radius. Recently, Tjahjadi *et al* [15] have undertaken an experimental and numerical study of the breakup of viscous cylindrical threads of one fluid into another. The experiments and the computations show that at the time of breakup the jet tends to form larger primary drops joined to smaller satellite drops. It is precisely this regime that we can describe theoretically with excellent qualitative agreement with both computations and experiments. Besides their intrinsic interest, such solutions can be useful in providing initial conditions for the continuation of numerical solutions just before the change in topology necessitated by the pinching. The analytical description of local structures is also useful in the determination of the effect of additional physicochemical effects such as surface-active agents or electrical forces on the pinching process. More recently, Eggers [16] provided a comprehensive review on nonlinear dynamics and breakup of free-surface flows where the author discussed the theoretical development of this field alongside experimental work, and outlined unsolved problems.

Currently there is a considerable amount of literature available on Newtonian liquid jet instability. However, things are more difficult for viscoelastic jets caused by the complex nature of the constitutive behavior of such a liquid [17–23]. The axisymmetric instability of non-Newtonian jets was studied by Sterling and Sleicher [20], Lin and Lian [21], Lin and Ibrahim [22], Brenn *et al* [23], Liu and Liu [24]. Liu and Liu [24] extended the work on Newtonian jets done by Li [25] to investigate the mechanisms of temporal instability of viscoelastic liquid jets with both axisymmetric and asymmetric disturbances, and to explore the differences between the instabilities of axisymmetric and asymmetric disturbances, concentrating on the wind-induced regime. Goren and Gottlieb [26] showed that the effect of the non-Newtonian liquid behavior may be described by a linear analysis when an unrelaxed axial tension is included in the momentum equation. This leads to an additional term in the dispersion relation that depends on a non-dimensional elastic tension parameter. Nevertheless, relatively few authors have studied jet instability caused by spatial variations of surface tension, despite the practical relevance of this phenomenon [27]. As pointed out by Furlani [27], advances

in micro-electro-mechanical system (MEMS) technology have enabled the development of a microfluidic inkjet printhead with thousands of nozzles that are thermally modulated near the nozzle orifice to produce steady steams of picoliter-sized droplets at kilo-Hertz frequency rates [27–31]. The ink delivery channel is pressurized and liquid streams are formed from the jet nozzle. The thermal energy imparted to the jet is carried downstream by its velocity. Because the surface tension of the jet is temperature dependent, the thermal modulation gives rise to a time-dependent spatial variation of surface tension along the free surface. Because a liquid with a high surface tension pulls more strongly on the surrounding liquid than one with a low surface tension, the presence of a gradient in surface tension will naturally cause the liquid to flow away from regions of low surface tension, thereby inducing a Marangoni flow toward regions of higher surface tension. Such a Marangoni flow produces a deformation of the free surface that ultimately leads to jet breakup and drop formation at a certain distance above the jet nozzle. The energy supplied to the heater is in the form of an electrical pulse train. To achieve synchronous drop breakup, only a very small amount of energy is needed ($<$1 nJ). The drop size may be precisely controlled by the delay time between the heater pulses (in conjunction with the orifice diameter and ink flow rate, which is controlled by the applied pressure).

Furlani [27] studied the temporal instability of an infinite Newtonian microjet that is subjected to a spatially periodic variation of surface tension along its length. A linear theory was developed for the temporal instability of such a liquid jet. The variation of surface tension induced Marangoni flow within the jet and led to breakup and drop formation. An analytical expression was derived for the behavior of the free surface of the jet. This expression was useful for parametric analysis of jet instability and breakup as a function of jet radius, wavelength and fluid properties.

The objective of the present paper is to investigate the mechanisms of temporal instability of non-Newtonian liquid jets, more specifically viscoelastic liquid jets, with a surface tension gradient. The constitutive behavior of the viscoelastic jets is represented by Oldroyd's model [32, 33]. The present work can provide a good foundation for further investigations of the instability and breakup of viscoelastic liquid jets under the situation where the surface tension gradient exits. As we mentioned earlier, applications of such a phenomenon include thermally driven inkjet. In the following sections, the dispersion relation between the growth rate and the wave number for a viscoelastic liquid jet will be derived. The effects of various parameters on the instability behavior are studied. Finally, a number of quantitative conclusions and sensitivities on the instability behavior of viscoelastic jets are investigated.

2. Mathematical formulation and solutions

Consider a cylindrical jet of viscoelastic liquid of density ρ, surface tension σ and an initial radius 'a', moving at velocity V_0 shown in figure 1. The governing equations are written in a cylindrical coordinate system for convenience. The coordinates are chosen such that the z-axis is parallel to the moving direction of the liquid jet flow; the r-axis is normal to the liquid jet with its origin located on the jet axis.

The governing equations of a liquid jet are the conservation laws for mass and momentum, i.e.,

$$\frac{\partial \rho}{\partial t} + \nabla \cdot \rho V = 0 \tag{1}$$

$$\rho \left(\frac{\partial}{\partial t} + V \cdot \nabla \right) V = -\nabla \cdot T, \tag{2}$$

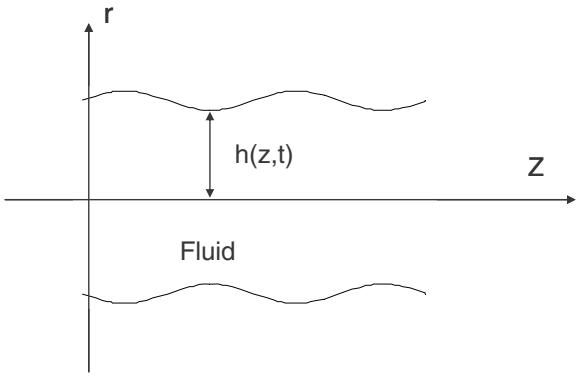

Figure 1. Liquid jet schematics where $h(z, t)$ defined the dynamic profile of the jet.

where t is time, V is the jet velocity vector, T is the total stress tensor given as $T = pI + \tau$; here p is the pressure in the fluid, $\boldsymbol{I}$ is the identity tensor and $\boldsymbol{\tau}$ is the viscous stress tensor of the fluid.

A set of constitutive equations is needed to relate stress and strain rate in order to solve equations (1) and (2). Here we utilize the 8-constant model developed by Oldroyd [32, 33]. The Oldroyd model is an empirical expression that is linear in the stress tensor, but contains all allowable products of stresses and velocity gradients. Because it can give qualitatively correct results in a wide variety of flow situations, it has been popular for developing the numerical techniques for non-Newtonian fluid dynamics. More discussion on the Oldroyd model and other models can be found in Bird *et al* [34].

The 8-constant Oldroyd model is written as

$$\tau + \lambda_1 \frac{\mathbf{D}\tau}{\partial t} + \frac{1}{2}\lambda_3\{\dot{\gamma}\cdot\tau + \tau\cdot\dot{\gamma}\} + \frac{1}{2}\lambda_5 \mathbf{tr}(\tau)\dot{\gamma} + \frac{1}{2}\lambda_6(\tau : \dot{\gamma})I = -\eta_0\left[\dot{\gamma} + \lambda_2\frac{\mathbf{D}\dot{\gamma}}{\partial t} + \lambda_4\{\dot{\gamma}\cdot\dot{\gamma}\} + \frac{1}{2}\lambda_7(\dot{\gamma} : \dot{\gamma})I\right],$$

where $\dot{\gamma} = (\nabla V)^T + \nabla V$ is the strain rate tensor, the superscript 'T' indicates the transpose, I is the unit tensor, $\frac{\mathbf{D}\tau}{\partial t}$ is the first contravariant convected time derivative, defined for the stress tensor τ as

$$\frac{\mathbf{D}\tau}{\partial t} = \frac{D\tau}{\mathrm{d}t} - \{(\nabla V)^T\cdot\tau + \tau\cdot(\nabla V)\}.$$

Here $\frac{D\tau}{\mathrm{d}t}$ is the material derivative of the stress tensor τ. Similarly, for strain rate, we have

$$\frac{\mathbf{D}\dot{\gamma}}{\partial t} = \frac{D\dot{\gamma}}{\mathrm{d}t} - \{(\nabla v)^T\cdot\dot{\gamma} + \dot{\gamma}\cdot(\nabla v)\}.$$

The eight constants in the Oldroyd model are zero shear stress viscosity, η_0 and the time constants $\lambda_1, \lambda_2, \ldots, \lambda_7$. The Oldroyd model can be reduced to the Newtonian model (when $\lambda_1 = \lambda_2 = \cdots = \lambda_7 = 0$), and other models such as the upper convected Maxwell model, Oldroyd-B model, second-order fluid model and Gordon–Schowalter model.

We neglect the nonlinear terms and gravitational effects and obtain the following equations for the incompressible flow:

$$\nabla\cdot V = 0 \tag{3}$$

$$\rho\left(\frac{\partial}{\partial t}+V_0\cdot\frac{\partial}{\partial z}\right)V=-\nabla\cdot(pI+\tau) \tag{4}$$

$$\tau+\lambda_1\left(\frac{\partial}{\partial t}+V_0\cdot\frac{\partial}{\partial z}\right)\tau=-\eta_0\left[\dot\gamma+\lambda_2\left(\frac{\partial}{\partial t}+V_0\cdot\frac{\partial}{\partial z}\right)\dot\gamma\right], \tag{5}$$

where $\dot\gamma$ is the strain tensor, η_0 is the zero shear viscosity, λ_1 is the stress relaxation time and λ_2 is the deformation retardation time.

We study the behavior of the jet when it is subjected to a perturbation. We represent the free surface of the perturbed jet by

$$h(z,t)=a+\delta(z,t), \tag{6}$$

where a is the radius of an unperturbed jet and $\delta(z,t)$ is the displacement of the free surface from the equilibrium position.

Because we are interested in the wave motion in the liquid, we seek the solutions for the velocity vector V as periodic functions in z and complex exponential functions in t, i.e.,

$$V_r=v_r(r)\,\mathrm{e}^{\mathrm{i}kz+\alpha t} \tag{7}$$

$$V_z=v_z(r)\,\mathrm{e}^{\mathrm{i}kz+\alpha t}, \tag{8}$$

where α is a frequency whose real part represents the wave growth rate of the disturbance, α is 2π times the disturbance frequency, and $-\alpha/k$ is the wave propagation velocity of the disturbance in the direction of the liquid flow, and k represents the wave number of the disturbance in the z direction.

The viscous stress tensor τ, the strain tensor $\dot\gamma$, the pressure p and the surface displacement δ are periodic functions in z and exponential functions in t, i.e.,

$$\tau=T(r)\,\mathrm{e}^{\mathrm{i}kz+\alpha t} \tag{9}$$

$$\dot\gamma=\dot\Gamma(r)\,\mathrm{e}^{\mathrm{i}kz+\alpha t} \tag{10}$$

$$p=P(r)\,\mathrm{e}^{\mathrm{i}kz+\alpha t} \tag{11}$$

$$\delta=\delta_0\,\mathrm{e}^{\mathrm{i}kz+\alpha t}, \tag{12}$$

where δ_0 is the initial amplitude of the disturbance, which is thought to be much smaller than the radius a of the jet in the linear stability theory.

Substituting equations (9) and (10) into equation (5), one has

$$\tau=-\eta(\alpha)\dot\gamma \tag{13}$$

where

$$\eta(\alpha)=\eta_0\frac{1+\lambda_2(\alpha+\mathrm{i}kV_0)}{1+\lambda_1(\alpha+\mathrm{i}kV_0)}. \tag{14}$$

Utilizing equation (13) and expressing the governing equations and the velocity vector in suitable component forms, the momentum equations are obtained in cylindrical coordinates:

$$\rho\left(\frac{\partial V_r}{\partial t}+V_0\frac{\partial V_r}{\partial z}\right)=-\frac{\partial p}{\partial r}+\eta(\alpha)\left\{\frac{\partial}{\partial r}\left[\frac{1}{r}\frac{\partial}{\partial r}(rV_r)\right]+\frac{\partial^2V_r}{\partial z^2}\right\} \tag{15}$$

$$\rho\left(\frac{\partial V_z}{\partial t}+V_0\frac{\partial V_z}{\partial z}\right)=-\frac{\partial p}{\partial z}+\eta(\alpha)\left\{\frac{1}{r}\frac{\partial}{\partial r}\left(r\frac{\partial V_z}{\partial r}\right)+\frac{\partial^2V_z}{\partial z^2}\right\}. \tag{16}$$

And the scalar continuity is given as

$$\frac{1}{r}\frac{\partial}{\partial r}(rV_r) + \frac{\partial V_z}{\partial z} = 0. \tag{17}$$

The flow field solutions of the above governing equations must satisfy the kinematic and dynamic boundary conditions at the liquid surface, which can be taken to be $r = a$ (the first-order approximation for a small displacement of the interface that is due to the disturbance). Thus, in mathematical form, the kinematic boundary condition requires that

$$V_r|_{r=h} = \left\{\frac{\partial \delta}{\partial t} + V_0\frac{\partial \delta}{\partial z}\right\}\Bigg|_{r=h} \tag{18}$$

and the dynamic boundary conditions require that

$$\tau_{rz}|_{r=h} = -\eta(\alpha)\left\{\frac{\partial V_z}{\partial r} + \frac{\partial V_r}{\partial z}\right\}\Bigg|_{r=h} = \frac{\partial \sigma(z)}{\partial z} \tag{19}$$

$$(p + \tau_{rr})|_{r=h} + p_\sigma = \left\{p - 2\eta(\alpha)\frac{\partial V_r}{\partial r}\right\}\Bigg|_{r=h} + p_\sigma = 0, \tag{20}$$

where

$$p_\sigma = \frac{\sigma_0}{a^2}\left(\delta + a^2\frac{\partial^2 \delta}{\partial z^2}\right) = \frac{\sigma_0}{a^2}(1 - k^2a^2)\delta_0\, \mathrm{e}^{\mathrm{i}kz+\alpha t} \tag{21}$$

is the pressure induced by the surface tension, the gradient of surface tension, $\sigma(z) = \sigma_0 + \Delta\sigma(1 + \mathrm{e}^{\mathrm{i}kz})\,\mathrm{e}^{\alpha t}$ produces a marangoni flow toward regions of higher surface tension which deform the free surface of the jet and ultimately causes jet breakup. In the expression of $\sigma(z)$, σ_0 is the unperturbed surface tension of the liquid, $\Delta\sigma$ is a parameter representing the magnitude of the surface tension disturbance.

Substituting equations (7), (8) and (11) into equations (15), (16), and (17), one can reduce the partial differential equations (15) to (17) into three ordinary differential equations with respect to a single variable r. These ordinary differential equations can be solved with the boundary conditions outlined in equations (19) and (20). The solutions are in the forms of Bessel functions given below:

$$V_r = \left\{\left[l^2 + k^2 - \frac{k^2\Delta\sigma\rho}{(k^2 - l^2)\eta(\alpha)^2\delta_0}\right]\frac{I_1(kr)}{I_1(ka)} - \left[2k^2 - \frac{k^2\Delta\sigma\rho}{(k^2 - l^2)\eta(\alpha)^2\delta_0}\right]\frac{I_1(lr)}{I_1(la)}\right\}\frac{\eta(\alpha)}{\rho}\delta_0\,\mathrm{e}^{\mathrm{i}kz+\alpha t} \tag{22}$$

$$V_z = \mathrm{i}\left\{\left[l^2 + k^2 - \frac{k^2\Delta\sigma\rho}{(k^2 - l^2)\eta(\alpha)^2\delta_0}\right]\frac{I_0(kr)}{I_1(ka)} - \left[2kl - \frac{kl\Delta\sigma\rho}{(k^2 - l^2)\eta(\alpha)^2\delta_0}\right]\frac{I_0(lr)}{I_1(la)}\right\}\frac{\eta(\alpha)}{\rho}\delta_0\,\mathrm{e}^{\mathrm{i}kz+\alpha t} \tag{23}$$

$$p = -\left[l^2 + k^2 - \frac{k^2\Delta\sigma\rho}{(k^2 - l^2)\eta(\alpha)^2\delta_0}\right]\frac{I_0(kr)}{kI_1(ka)}\frac{\eta(\alpha)}{\rho}(\alpha + \mathrm{i}kV_0)\delta_0\,\mathrm{e}^{\mathrm{i}kz+\alpha t}, \tag{24}$$

where

$$l^2 = k^2 + \frac{\rho(\alpha + \mathrm{i}kV_0)}{\eta(\alpha)}. \tag{25}$$

The growth rate equation is derived from the normal stress condition, equation (20), using equations (14), (21), (22) and (24). After some algebra, we find that

$$-\delta_0\eta^2(k^2+l^2)^2\frac{I_0(ak)}{k\rho I_1(ak)}+\Delta\sigma k(k^2+l^2)\frac{I_0(ak)}{(k^2-l^2)I_1(ak)}$$
$$+4\delta_0\eta^2k^2l\frac{I_0(al)}{\rho I_1(al)}-2\Delta\sigma k^2l\frac{I_0(al)}{(k^2-l^2)I_1(al)}$$
$$=\frac{\delta_0[2a\eta^2(k^2-l^2)-\rho(1-a^2k^2)\sigma_0]}{\rho a^2}. \tag{26}$$

Equation (26) can be written in terms of the ratio of surface tension disturbance and jet radius, i.e. $\frac{\Delta\sigma}{\delta_0}$

$$-\eta^2(k^2+l^2)^2\frac{I_0(ak)}{k\rho I_1(ak)}+\frac{\Delta\sigma}{\delta_0}k(k^2+l^2)\frac{I_0(ak)}{(k^2-l^2)I_1(ak)}$$
$$+4\eta^2k^2l\frac{I_0(al)}{\rho I_1(al)}-2\frac{\Delta\sigma}{\delta_0}k^2l\frac{I_0(al)}{(k^2-l^2)I_1(al)}$$
$$=\frac{2a\eta^2(k^2-l^2)-\rho(1-a^2k^2)\sigma_0}{\rho a^2}. \tag{27}$$

For inviscid liquid and when $\Delta\sigma=0$, $\eta^2\,(k^2+l^2)^2\to\rho^2\alpha^2$, therefore, equation (27) gives

$$\alpha^2=\frac{\sigma_0}{\rho a^3}ka(1-k^2a^2)\frac{I_1(al)}{I_0(al)}, \tag{28}$$

which is Rayleigh's result [1] for an inviscid liquid jet in a vacuum.

Now we search for a relationship between $\Delta\sigma$ and δ_0. The kinematic boundary condition requires that fluid does not cross the free surface,

$$\frac{D}{Dt}(r-\delta(z,t))=0 \qquad \text{at the free surface boundary } r=h, \tag{29}$$

which can be written as

$$\frac{\partial\delta}{\partial t}+V_z\frac{\partial\delta}{\partial z}=V_r. \tag{30}$$

Let

$$V_z=V_z^0(z,t)+O(r), \tag{31}$$

then from the continuity condition, equation (17), we have

$$V_r=-\frac{1}{2}\frac{\partial}{\partial z}V_z^0(z,t)r+O(r^2). \tag{32}$$

Substituting equations (31) and (32) into equation (30) and ignoring the higher order terms in r, we have

$$\frac{\partial\delta}{\partial t}+V_0\frac{\partial\delta}{\partial z}=-\frac{1}{2}\frac{\partial}{\partial z}V_z^0(z,t)a. \tag{33}$$

Using equation (23) and letting r approach to a, we have

$$V_z^0(z,t)=\mathrm{i}\left\{\left[l^2+k^2-\frac{k^2\Delta\sigma\rho}{(k^2-l^2)\eta(\alpha)^2\delta_0}\right]-\left[2kl-\frac{kl\Delta\sigma\rho}{(k^2-l^2)\eta(\alpha)^2\delta_0}\right]\right\}\frac{\eta(\alpha)}{\rho}\delta_0\,\mathrm{e}^{\mathrm{i}kz+\alpha t}. \tag{34}$$

Substituting equations (12) and (34) into equation (33), we have an equation that determines the relationship between $\Delta\sigma$ and δ_0, which reduces to

$$\frac{\Delta\sigma}{\delta_0}=\frac{\eta(k^2-l^2)\{a\eta k(k^2+l^2)I_1(al)-2I_1(ak)[a\eta k^3+(\alpha+\mathrm{i}kV_0)\rho I_1(al)]\}}{ak^3\rho[I_1(al)-I_1(ak)]}. \tag{35}$$

Using equation (35), we rewrite equation (27) as

$$\alpha^2\rho I_0(ak)[ak - 2I_1(al)] + 2\eta k\alpha\{lI_0(al)[2I_1(ak) - ak] - kI_0(ak)[2I_1(al) - ak] + k[I_1(al) - I_1(ak)]\} = \frac{(1 - a^2k^2)k^2\sigma_0[I_1(ak) - I_1(al)]}{a}. \tag{36}$$

Equations (27) and (34), or equation (36) define the growth rate of the jet. Equation (36) can be expressed in a dimensionless form as

$$\bar{\alpha}^2 I_0(ak)[ak - 2I_1(al)] + 2akZ\bar{\alpha}\frac{Z + \bar{\lambda}El\bar{\alpha}}{Z + El\bar{\alpha}}\{alI_0(al)[2I_1(ak) - ak] - akI_0(ak)[2I_1(al) - ak] + ak[I_1(al) - I_1(ak)]\} = (1 - a^2k^2)a^2k^2[I_1(ak) - I_1(al)], \tag{37}$$

where

$$\bar{\alpha} = \frac{\alpha}{\sqrt{\sigma_0/(\rho a^3)}}, \qquad Z = \frac{\eta_0}{\sqrt{\sigma_0\rho a}}, \qquad El = \frac{\eta_0\lambda_1}{\rho a^2}, \qquad \bar{\lambda} = \frac{\lambda_2}{\lambda_1}. \tag{38}$$

Here $\bar{\alpha}$ is the non-dimensional growth rate, Z is the Ohnersorge number that denotes the ratio of viscous forces to surface tension force, El is the elastic number which was introduced by Kroesser and Middleman [35] and later utilized by Brenn *et al* [23]. The parameter, El represents a ratio of viscous and elastic time of the liquid jet. The parameter $\bar{\lambda}$ denotes the ratio of deformation retardation to stress relaxation time. According to Bird *et al* [34], the values of $\bar{\lambda}$ are between 1/9 and 1. It should also be pointed out that ak is the dimensionless wave number, al can be expressed by the dimensionless parameters in equation (38) as

$$al = \sqrt{(ak)^2 + \frac{\bar{\alpha}}{Z}\frac{Z + El\,\bar{\alpha}}{Z + \bar{\lambda}El\,\bar{\alpha}}}. \tag{39}$$

By setting $\Delta\sigma$ equal to zero in equation (27) and utilizing the dimensionless parameters defined in equation (38), the dimensionless dispersion equation for zero surface tension gradient is obtained as

$$\left[Z\frac{Z + \bar{\lambda}El\,\bar{\alpha}}{Z + El\,\bar{\alpha}}\right]^2\left\{2(ak)^2\left[1 - \left(\frac{al}{ak}\right)^2\right] + (ak)^3\left[1 + \left(\frac{al}{ak}\right)^2\right]^2\frac{I_0(ak)}{I_1(ak)} - 4(ak)^2(al)\frac{I_0(al)}{I_1(al)}\right\} = 1 - (ak)^2. \tag{40}$$

3. Results and discussion

In figure 2 we consider the normalized growth rate, $\bar{\alpha}$, determined from equation (37), of a jet of Separan AP30 solution (aqueous 0.05%). According to the definition given in equations (7)–(11), the growth rate α represents how fast the velocity and radius of the jet change as a function of time. Separan is a polyacrylamide frequently used in experiments on viscoelastic jets. The parameters for the jets are as follows: $a = 9.21 \times 10^{-4}$ m, $\rho = 1000$ kg m^{-3}, $\sigma_0 = 70.5 \times 10^{-3}$ N m^{-1}, $\eta_0 = 0.11$ N s m^{-2}, $\lambda_1 = 0.01$ s and $\lambda_2 = 0.01$ s. The jet is subjected to a surface tension gradient along the jet, which produces a Marangoni flow toward regions of higher surface tension. There also exists an initial disturbance of jet radius, with magnitude δ_0. Both of these effects further deform the free surface of the jet and ultimately lead to jet breakup. The dashed line is the growth rate prediction when the spatial variation of surface tension along the length of the jet is considered. The solid line is the growth rate prediction

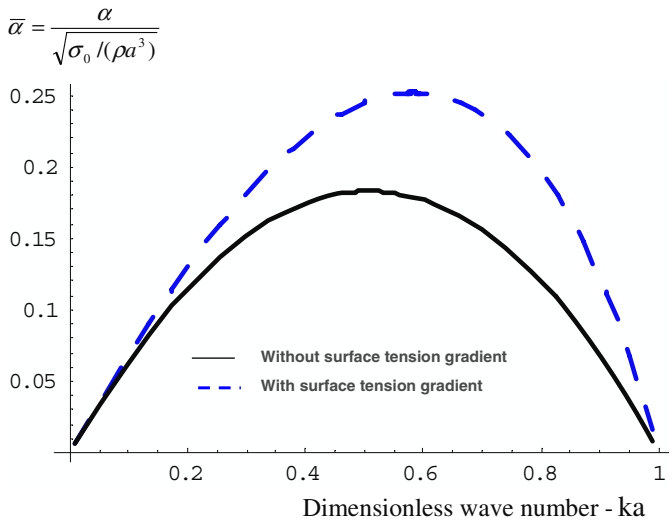

Figure 2. Normalized growth rate, $\bar{\alpha}$ as a function of dimensionless wave number, ka. The parameters are: $a = 9.21 \times 10^{-4}$ m, $\rho = 1000$ kg m^{-3}, $\sigma_0 = 70.5 \times 10^{-3}$ N m^{-1}, $\eta_0 = 0.11$ N s m^{-2}, $\lambda_1 = 0.01$ s , $\lambda_2 = 0.01$ s, which yield corresponding dimensionless parameters as $Z = 0.4317$, $El = 1.2968$, $\bar{\lambda} = 1$.

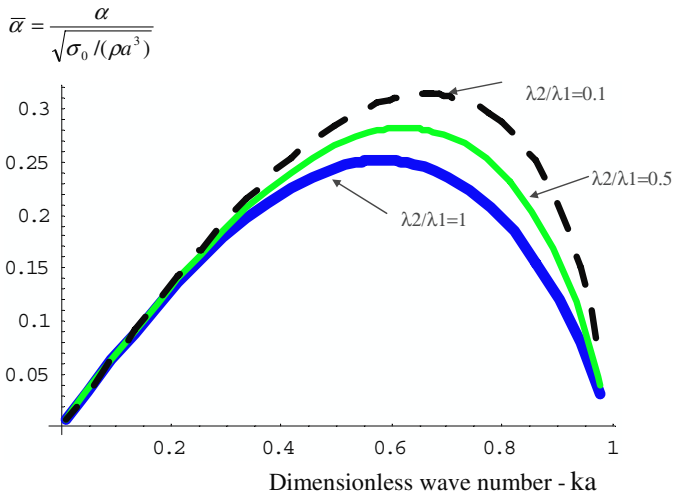

Figure 3. The effect of time constant ratio $\bar{\lambda}$ on normalized growth rate, $\bar{\alpha}$ as a function of dimensionless wave number, ka. The parameters are: $a = 9.21 \times 10^{-4}$ m , $\rho = 1000$ kg m^{-3} , $\sigma_0 = 70.5 \times 10^{-3}$ N m^{-1}, $\eta_0 = 0.11$ N s m^{-2} and $\lambda_1 = 0.01$ s. The corresponding dimensionless parameters are $Z = 0.4317$ and $El = 1.2968$.

when the spatial variation of surface tension along the length of the jet is not considered. It is clear that the addition of the gradient of surface tension produces a higher growth rate and thus a shorter breakup time.

The effect of the stress relaxation time λ_1 and deformation retardation time λ_2 on growth rate is shown in figure 3, presented in terms of $\frac{\lambda_2}{\lambda_1}$. The curve for $\frac{\lambda_2}{\lambda_1} = 1$ is identical to that

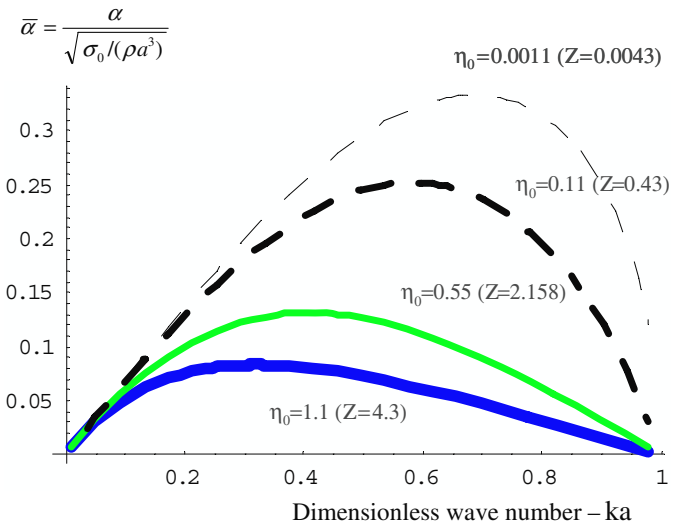

Figure 4. Effect of viscosity on normalized growth rate for a Newtonian jet. The parameters are: $a = 9.21 \times 10^{-4}$ m, $\rho = 1000$ kg m^{-3}, $\sigma_0 = 70.5 \times 10^{-3}$ N m^{-1} and $\lambda_1 = \lambda_2 = 0$. *El* is 0 and *Z* are given inside the plot.

of a Newtonian jet with the same viscosity (0.11 N s m^{-2}). The parameters for the jet are as follows: $a = 9.21 \times 10^{-4}$ m, $\rho = 1000$ kg m^{-3}, $\sigma_0 = 70.5 \times 10^{-3}$ N m^{-1}, $\eta_0 = 0.11$ N s m^{-2} and $\lambda_1 = 0.01$ s.

The effect of the viscosity on the growth rate of a Newtonian jet is shown in figure 4. The parameters for the jet are as follows: $a = 9.21 \times 10^{-4}$ m, $\rho = 1000$ kg m^{-3}, $\sigma_0 = 70.5 \times 10^{-3}$ N m^{-1}, $\lambda_1 = 0.1$ s and $\lambda_2 = 0$. It is seen from figure 4 that growth rate decreases with increasing viscosity or the Ohnersorge number. Furthermore, the maximum growth rate occurs at a different value of wave number as well. For example, when viscosity is equal to 1.1×10^{-3} N s m^{-2}, the maximum growth rate occurs at wave number $k = 0.7$. When viscosity is equal to 0.11 N s m^{-2}, the maximum growth rate shifts left, occurring at wave number $k = 0.58$. When viscosity is equal to 1.1 N s m^{-2}, the maximum growth rate shifts further left, occurring at wave number $k = 0.32$.

The effect of the initial viscosity on the growth rate of a non-Newtonian jet is shown in figure 5. The parameter for the jet are as follows: $a = 9.21 \times 10^{-4}$ m, $\rho = 1000$ kg m^{-3}, $\sigma_0 = 70.5 \times 10^{-3}$ N m^{-1}, $\lambda_1 = 0.1$ s and $\lambda_2 = 0.01$ s. Similar to the results for a Newtonian jet shown in figure 5, the growth rate of a non-Newtonian jet decreases with increasing viscosity or the Ohnersorge number, and the maximum growth rate occurs at a different value of wave number. In figure 6, we compare the wave number for maximum growth rate for both Newtonian and non-Newtonian jets at various values of viscosity. For a non-Newtonian jet, the wave number for maximum growth rate decreases slower with increasing viscosity.

Equation (14) can be written as

$$\eta(\alpha) = \eta_0 \frac{1 + \lambda_2 \alpha_S}{1 + \lambda_1 \alpha_S} \approx \begin{cases} \eta_0\left(\frac{\lambda_2}{\lambda_1}\right), & \text{when} \quad \lambda_2 \alpha_S \gg 1, \lambda_1 \alpha_S \gg 1 \\ \eta_0, & \text{when} \quad \lambda_2 \alpha_S \ll 1, \lambda_1 \alpha_S \ll 1 \end{cases} \tag{41}$$

where $\alpha_S = \alpha + \mathrm{i}kV_0$ and α is the growth rate in a coordinate system fixed with the moving jet. Equation (41) indicates that when the product of growth rate and the stress relaxation time λ_1, and the product of growth rate and deformation retardation time λ_2 are both much larger than 1,

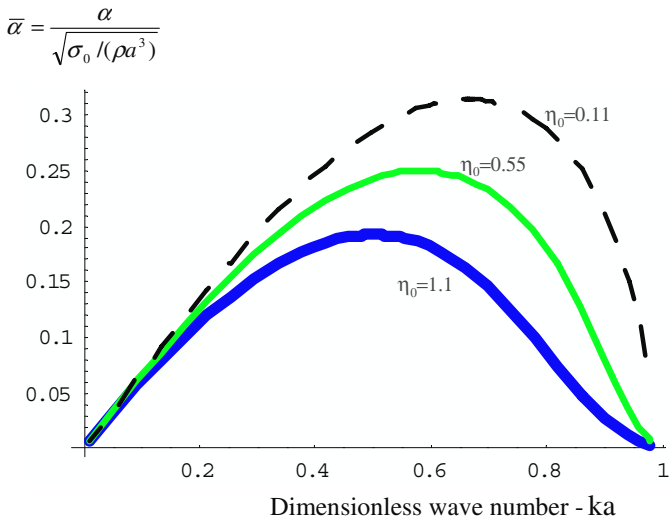

Figure 5. Effect of viscosity on growth rate for a non-Newtonian jet. The parameters are: $a = 9.21 \times 10^{-4}$ m, $\rho = 1000$ kg m^{-3}, $\sigma_0 = 70.5 \times 10^{-3}$ N m^{-1}, $\lambda_1 = 0.1$ s and $\lambda_2 = 0.01$ s. The corresponding dimensionless parameters are: $\bar{\lambda} = 0.1$ and $Z = 0.43$, $El = 12.97$ for $\eta_0 = 0.11$, $Z = 2.158$, $El = 64.85$ for $\eta_0 = 0.55$, and $Z = 4.37$, $El = 129.68$ for $\eta_0 = 1.1$.

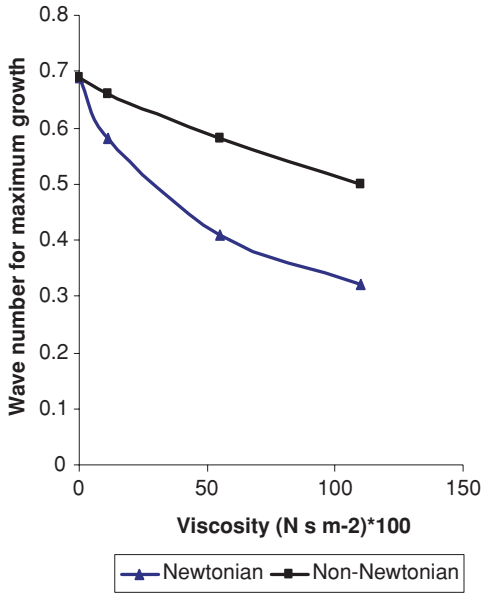

Figure 6. Effect of viscosity (normalized wave number) on location of maximum growth rate. The parameters are given in figure 4 for the Newtonian liquid and in figure 5 for non-Newtonian liquid.

the jet behaves like a Newtonian fluid with its viscosity modified as $\eta = \eta_0\left(\frac{\lambda_2}{\lambda_1}\right)$. Furthermore, $\eta = \eta_0$ when $\lambda_2 = \lambda_1$ or when the product of growth rate and the stress relaxation time, and the product of growth rate and the deformation retardation time are both much smaller than 1.

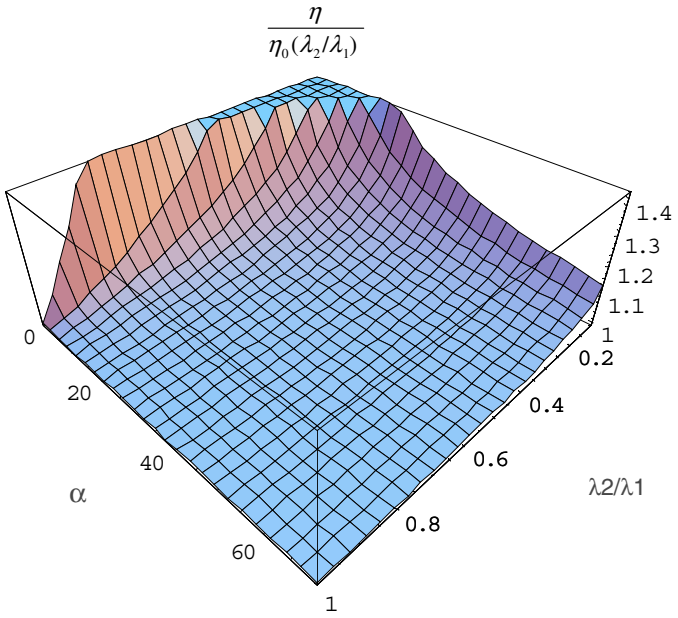

Figure 7. Normalized viscosity as a function of growth rate and relaxation and retardation rate.

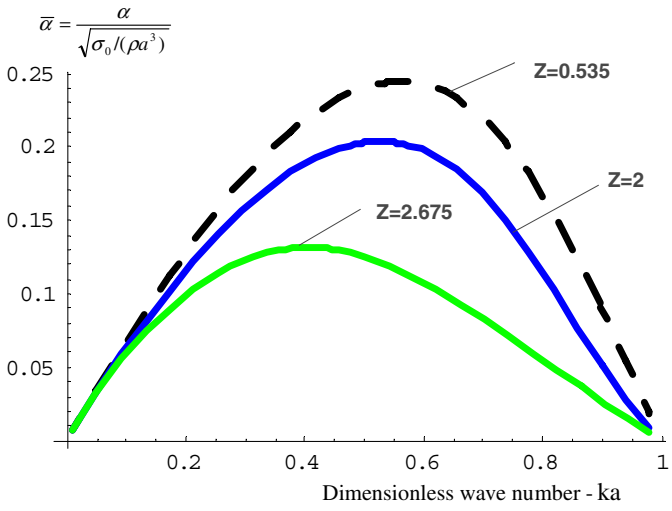

Figure 8. Normalized growth rate, $\bar{\alpha}$ as a function of dimensionless wave number, *ka*. The dimensionless parameters as $El = 4$ and $\bar{\lambda} = 0.1$.

Figure 7 shows the apparent viscosity η, normalized by $\eta_0\left(\frac{\lambda_2}{\lambda_1}\right)$ as a function of α_S and $\frac{\lambda_2}{\lambda_1}$. It is clear that for most of the range of variables considered, the normalized apparent viscosity is close to 1.

In figure 8, the sensitivity of the normalized growth rate to the Ohnersorge number Z is presented. The elastic number El is equal to 4. The ratio of deformation retardation to stress relaxation time $\bar{\lambda}$ is equal to 0.1. Since the Ohnersorge number denotes the ratio of viscous

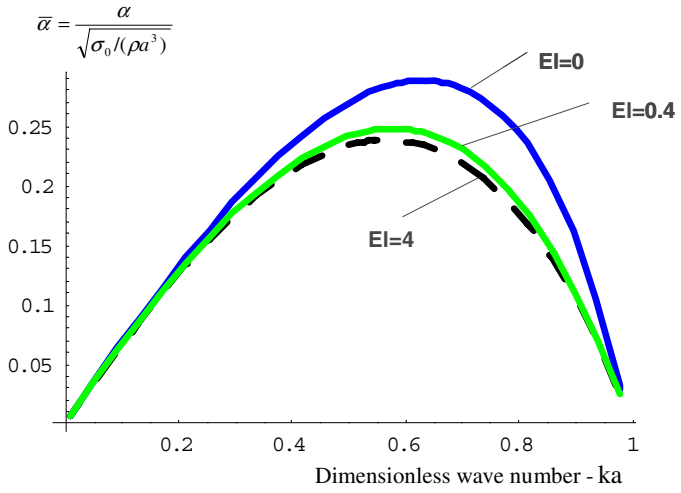

Figure 9. Normalized growth rate, $\bar{\alpha}$ as a function of dimensionless wave number, *ka*. The dimensionless parameters as $Z = 0.535$ and $\bar{\lambda} = 0.1$.

forces to surface tension force, a smaller Ohnersorge number indicates a smaller viscous force in comparison to the surface tension force. Figure 8 shows that in such a case (smaller *Z*) the normalized growth rate is higher. This makes sense since surface tension is responsible for driving the jet breakup.

In figure 9, the sensitivity of the normalized growth rate to the elastic number *El* is presented. The Ohnersorge number *Z* is equal to 0.535. The ratio of deformation retardation to stress relaxation time $\bar{\lambda}$ is equal to 0.1. The elastic number *El* represents the ratio of viscous and elastic time of the liquid jet. Figure 9 shows that a smaller elastic number yields a higher normalized growth rate.

We emphasize that slender jet theories are powerful methods in the description of local structures in pinching phenomena. In capillary instability phenomena in three dimensions, slender jet theories provide simplified sets of evolution equations which can be analyzed for breakup. The present approach corresponds to a different physical setup. If the jet is allowed to undergo natural growth without any external forces and linear waves are at first important, then linear theory can be used to predict a maximally growing wave. As mentioned above, this wave has wavelength in the order of the undisturbed jet radius, so when the evolution enters the nonlinear regime, the interfacial waves have axial length scales comparable to the undisturbed jet radius. The slender jet approximation may not be appropriate, therefore, for the *total* duration of the evolution to breakup, even though it is appropriate locally at breakup.

Acknowledgments

The author thanks Dr Ed Furlani and Dr Gil Hawkins for valuable technical discussions.

References

[1] Rayleigh L 1878 On the instability of jets *Proc. Lond. Math. Soc.* **10** 4–13
[2] Rayleigh L 1899 *Scientific Papers* vol I (London: Cambridge University Press) p 361
[3] Lee H C 1974 Drop formation in a liquid jet *IBM J. Res. Dev.* **18** 364

[4] Levich V I 1962 *Physicochemical Hydrodynamics* (Englewood Cliffs, NJ: Prentice-Hall) p 361
[5] Rutland D F and Jameson G J 1970 Theoretical prediction of the sizes of drops formed in the breakup of capillary jets *Chem. Eng. Sci.* **25** 1689
[6] Goedde E F and Yuen M C 1970 Experiments on liquid jet instability *J. Fluid Mech.* **40** 495–511
[7] Kowalewski T A 1996 On the separation of droplets from a liquid jet *Fluid Dyn. Res.* **17** 121
[8] Peregrine D H, Shoker G and Symon A 1990 The bifurcation of liquid bridges *J. Fluid Mech.* **212** 25
[9] Yuen M-C 1968 Nonlinear capillary instability of a liquid jet *J. Fluid Mech.* **33** 151–63
[10] Chaudhary K C and Redekopp L G 1980 The nonlinear capillary instability of a liquid jet: Part 1. Theory *J. Fluid Mech.* **96** 257–74
[11] Bogy D B 1979 Drop formation in a circular liquid jet *Ann. Rev. Fluid Mech.* **11** 207–28
[12] Mansour N and Lundgren T S 1990 Satellite formation in capillary jet breakup *Phys. Fluids A* **2** 1141–4
[13] Tomotika S 1935 On the stability of a cylindrical thread of a viscous liquid surrounded by another viscous fluid *Proc. R. Soc. Lond.* A **150** 322–37
[14] Chandrasekhar S 1961 *Hydrodynamic and Hydromagnetic Stability* (Oxford: Clarendon)
[15] Tjahjadi M, Stone H A and Ottino J M 1992 Satellite and subsatellite formation in capillary breakup *J. Fluid Mech.* **243** 297–317
[16] Egger J 1997 Nonlinear dynamics and breakup of free-surface flows *Rev. Mod. Phys.* **69** 865–929
[17] Darby R 1976 *Viscoelastic Fluids* (New York: Dekker)
[18] Schowalter W R 1978 *Mechanics of Non-Newtonian Fluids* (Oxford: Pergamon)
[19] Yarin A L 1993 *Free Liquid Jets and Films: Hydrodynamics and Rheology* (New York: Wiley)
[20] Sterling A M and Sleicher C A 1975 The instability of capillary jets *J. Fluid Mech.* **68** 477–95
[21] Lin S P and Lian Z W 1990 Mechanism of the breakup of liquid jets *AIAA J.* **28** 120–26
[22] Lin S P and Ibrahim E A 1990 Instability of a viscous liquid jet surrounded by a viscous gas in a vertical pipe *J. Fluid Mech.* **218** 641–58
[23] Brenn G, Liu Z and Durst F 2000 Linear analysis of the temporal instability of axisymmetrical non-Newtonian liquid jets *Int. J. Multiph. Flow* **26** 1621–44
[24] Liu Z and Liu Z 2006 Linear analysis of three-dimensional instability of non-Newtonian liquid jets *J. Fluid Mech.* **559** 451–9
[25] Li X 1995 Mechanism of atomization of a liquid jet *Atomization Sprays* **5** 89–105
[26] Goren S and Gottlieb M 1982 Surface–tension-driven breakup of viscoelastic liquid threads *J. Fluid Mech.* **120** 245–66
[27] Furlani E P 2005 Temporal instability of viscous liquid microjets with spatially varying surface tension *J. Phys. A: Math. Gen.* **38** 263–76
[28] Chwalek J M *et al* 2002 A new method for deflecting liquid microjets *Phys. Fluids* **14** 37
[29] Furlani E P, Delametter C N, Chwalek J M and Trauernicht D P 2001 Surface tension induced instability of viscous liquid jets *Tech. Proc. 4th Int. Conf. on Modeling and Simulation of Microsystems* (Cambridge, MA: Applied Computational Reseasrch Society) p 186
[30] Chwalek J M, Trauernicht D P, Delametter C N, Jeanmaire D L and Anagnostopoulos C 2001 Novel silicon-based continuous inkjet printhead employing asymmetric heating deflection means *Tech. Proc. IS&T Non-Impact Printing* (NIP17) Technologies Conference
[31] Chwalek J M *et al* 2000 *US Patent* 6079821
[32] Oldroyd J G 1958 Non-Newtonian effects in steady motion of some idealized elastico-viscous liquids *Proc. R. Soc. Lond.* A **245** 278–97
[33] Oldroyd J G 1961 The hydrodynamics of materials whose rheological properties are complicated *Rheol. Acta* **1** 337–44
[34] Bird R B, Armstrong R C and Hassager O 1977 *Dynamics of Polymeric Liquids Fluid Mechanics* vol 1 (New York: Wiley)
[35] Kroesser F W and Middleman S 1969 Viscoelastic jet stability *AIChE J.* **15** 383–678